JOURNAL OF VIROLOGY, Mar. 2011, p. 2589–2598 Vol. 85, No. 6
0022-538X/11/$12.00 doi:10.1128/JVI.02260-10

Factors Supporting Intrathecal Humoral Responses following Viral Encephalomyelitis▽

Timothy W. Phares,[1] Cristina P. Marques,[1] Stephen A. Stohlman,[1] David R. Hinton,[2] and Cornelia C. Bergmann[1]*

Department of Neurosciences, NC30, Lerner Research Institute, Cleveland Clinic, 9500 Euclid Avenue, Cleveland, Ohio 44195,[1] *and Department of Pathology, Keck School of Medicine, University of Southern California, Los Angeles, California 90033*[2]

Received 28 October 2010/Accepted 18 December 2010

Central nervous system (CNS) infections and autoimmune inflammatory disorders are often associated with retention of antibody-secreting cells (ASC). Although beneficial or detrimental contributions of ASC to CNS diseases remain to be defined, virus-specific ASC are crucial in controlling persistent CNS infection following coronavirus-induced encephalomyelitis. This report characterizes expression kinetics of factors associated with ASC homing, differentiation, and survival in the spinal cord, the prominent site of coronavirus persistence. Infection induced a vast, gamma interferon (IFN-γ)-dependent, prolonged increase in chemokine (C-X-C motif) ligand 9 (CXCL9), CXCL10, and CXCL11 mRNA, supporting a role for chemokine (C-X-C motif) receptor 3 (CXCR3)-mediated ASC recruitment. Similarly, CD4 T cell-secreted interleukin-21, a critical regulator of both peripheral activated B cells and CD8 T cells, was sustained during viral persistence. The ASC survival factors B cell-activating factor of the tumor necrosis factor (TNF) family (BAFF) and a proliferating-inducing ligand (APRIL) were also significantly elevated in the infected CNS, albeit delayed relative to the chemokines. Unlike IFN-γ-dependent BAFF upregulation, APRIL induction was IFN-γ independent. Moreover, both APRIL and BAFF were predominantly localized to astrocytes. Last, the expression kinetics of the APRIL and BAFF receptors coincided with CNS accumulation of ASC. Therefore, the factors associated with ASC migration, differentiation, and survival are all induced during acute viral encephalomyelitis, prior to ASC accumulation in the CNS. Importantly, the CNS expression kinetics implicate rapid establishment, and subsequent maintenance, of an environment capable of supporting differentiation and survival of protective antiviral ASC, recruited as plasmablasts from lymphoid organs.

Virus-specific antibodies (Ab) play an important role in the control of many viral infections of the central nervous system (CNS) (17). Ab are delivered to the CNS either by diffusion across a compromised blood brain barrier (18, 53) or actively by Ab-secreting cells (ASC) which have infiltrated the CNS or differentiated locally in the inflamed tissue. Passage of Ab from serum is inefficient under steady-state conditions, making ASC-mediated Ab secretion at the site of CNS infection a more effective strategy of viral control. For example, Ab production by invading B cells is required to clear rabies virus from the CNS, as passively administered Ab do not mediate virus clearance (22). Furthermore, B cells in the CNS of Sindbis virus-infected mice continue to secrete Ab during viral RNA persistence, supporting the idea that ASC play a role in preventing viral recrudescence (71). In addition, prolonged intrathecal antiviral Ab production and ASC accumulation within the CNS occur following control of Semliki Forest virus (43, 53–55), measles virus (9, 48), and Theiler's murine encephalomyelitis virus (50, 51) infections.

The concept of an ASC survival niche in the CNS during chronic inflammatory disorders associated with autoimmunity is generally accepted. These ASC are thought to be derived from ectopic lymphoid follicle-like structures established *de novo* within the inflamed CNS (36, 63, 64). Following infection, virus-specific ASC accumulate in the CNS within 2 to 3 weeks postinfection (p.i.) and are distributed randomly throughout the tissue (43, 56, 70). However, ectopic lymphoid follicle-like structures have not been reported following viral CNS infections, suggesting that immature plasma cells traffic to the CNS from peripheral lymphoid germinal centers and subsequently differentiate and establish residence. This scenario requires expression of appropriate differentiation and survival factors within the CNS. Despite the common finding of ASC accumulation in the CNS during microbial infections in both experimental models and human diseases, the signals that contribute to ASC homing, differentiation, and maintenance, especially as they relate to the CNS, are poorly understood.

The present study defined the temporal expression of factors involved in fostering ASC recruitment, differentiation, and survival following sublethal coronavirus-induced encephalomyelitis. Infection of mice with the glia-tropic mouse hepatitis virus strain JHM (JHMV) is characterized by T cell-mediated control within 2 weeks, but viral RNA persists in spinal cords in the absence of detectable infectious virus. ASC recruitment into the CNS (69, 70) provides a local source of Ab controlling viral recrudescence (30, 58). Invading ASC initially exhibit an early plasmablast phenotype and, with time, progress to a more differentiated, sessile phenotype as indicated by diminishing major histocompatibility complex (MHC) class II expression (70). The crucial role of antiviral ASC within the CNS is evident by the transient nature of viral control following peripheral administration of JHMV-specific neutralizing Ab to

* Corresponding author. Mailing address: Department of Neurosciences, Lerner Research Institute, Cleveland Clinic, 9500 Euclid Avenue, NC30, Cleveland, OH 44195. Phone: (216) 444-5922. Fax: (216) 444-7927. E-mail: bergmac@ccf.org.

▽ Published ahead of print on 29 December 2010.

infected B cell-deficient mice (30, 58). Although T cells suffice to control acute viral replication and viral recrudescence can be delayed by Ab treatment, reemergence of infectious virus from very low levels of persisting viral RNA cannot be prevented as Ab levels wane (58). This report demonstrates induction and sustained expression of chemokines and differentiation and survival factors regulating humoral immunity in both CNS resident cells and infiltrating CD4 T cells. The temporal expression patterns suggest that all factors essential for ASC accumulation within the CNS are produced during acute CNS infection, while their sustained expression during persistence is more limited. Moreover, the findings that gamma interferon (IFN-γ) plays an essential role in enhancing expression of chemokine (C-X-C motif) receptor 3 (CXCR3) ligands and B cell-activating factor of the tumor necrosis factor (TNF) family (BAFF) but is dispensable for expression of interleukin-21 (IL-21) and a proliferating-inducing ligand (APRIL) imply flexibility in the mechanisms supporting intrathecal ASC in an infection model.

MATERIALS AND METHODS

Mice and infection. Wild-type (wt) C57BL/6 mice were purchased from the National Cancer Institute (Frederick, MD), while IFN-γ-deficient mice (IFN-$\gamma^{-/-}$) on the C57BL/6 background were previously described (52). Heterozygous mice expressing green fluorescent protein (GFP) via the B lymphocyte-induced maturation protein (BLIMP) promoter on the C57BL/6 background (Blimp-1-$GFP^{+/-}$) were kindly provided by Stephen Nutt, Institute of Medical Research, Parkville, Victoria, Australia. Six- to 7-week-old mice were infected intracranially with 250 PFU of the J.2.2v-1 monoclonal Ab variant of JHMV. Virus-specific B cells were elicited by intraperitoneal immunization with JHMV. All procedures were conducted in accordance with protocols approved by the Institutional Animal Care and Use Committee.

Flow cytometric analysis and fluorescence-activated cell sorting. For phenotypic analysis, CNS-derived mononuclear and splenic cells were isolated from pooled organs from 3 or 4 mice per time point as described previously (5). Expression of cell surface markers was determined by staining with Ab specific for CD4 (L3T4), CD8 (53-6.7), CD11b (M1/70), CD19 (1D3), CD45 (30-F11), CD138 (281-2) (BD Bioscience, San Jose, CA), and IgD (11-26) (eBioScience, San Diego, CA). Virus-specific CD8 T cells were identified using H2-D^b/S510 MHC class I tetramers (5). Cells were analyzed on a FACSCalibur flow cytometer (BD, Mountain View, CA) using FlowJo 7.1 software (Tree Star, Ashland, OR). Cell numbers were calculated based on cell yields and percentages of gated live cells. Splenic-derived naive B cells ($CD19^+$ $CD138^-$ IgD^+ GFP^-) and ASC ($CD19^{dim}$ $CD138^+$ IgD^- GFP^+) from both nonimmunized and JHMV-immunized mice were purified from pooled spleens ($n = 2$ or 3) using a BD FACSAria (BD Bioscience). Similarly, CNS monocyte-derived $CD45^{hi}$ $CD11b^+$ macrophages, $CD45^{lo}$ microglia, a $CD45^-$ $O4^-$-enriched astrocyte population, CD4 T cells, as well as tetramer-positive and tetramer-negative CD8 T cells were purified from pooled brains or spinal cords ($n = 6$ to 8). Oligodendroglia were gated out from the $CD45^-$ population using anti-O4 monoclonal Ab. The percentage of astrocytes in the enriched population is ~60% (76). A minimum of 10^5 cells collected per population were frozen in 400 μl of Trizol (Invitrogen, Carlsbad, CA) at −80°C for subsequent RNA extraction and PCR analysis as described previously (23).

Quantitative real-time PCR. Snap-frozen spinal cords or cervical lymph nodes (CLN) from individual mice ($n = 3$ or 4 per time point) were placed in Trizol and homogenized in glass grinders. RNA was isolated as described previously (23), and cDNA was synthesized using Moloney murine leukemia virus (M-MLV) reverse transcriptase (Invitrogen), oligo(dT) (Promega, Madison, WI) and random primers (Promega). Quantitative real-time PCR was performed using 4 μl of cDNA and SYBR green master mix (Applied Biosystems, Foster City, CA) in duplicate or triplicate on a 7500 fast real-time PCR system (Applied Biosystems). PCR conditions were as follows: 10 min at 95°C, followed by 40 cycles, where 1 cycle consists of 15 s at 95°C, 30 s at 60°C, and 30 s at 72°C. Real-time primer sequences were as follows: for glyceraldehyde-3-phosphate dehydrogenase (GAPDH), 5′-CATGGCCTTCCGTGTTCCTA-3′ (sense) and 5′-ATGCCTGC TTCACCACCTTCT-3′ (antisense); for interleukin-6 (IL-6), 5′-ACACATGTT CTCTGGGAAATCGT-3′ (sense) and 5′-AAGTGCATCATCGTTGTTCATA CA-3′ (antisense); for chemokine (C-X-C motif) ligand 9 (CXCL9), 5′-TGCA CGATGCTCCTGCA-3′ (sense) and 5′-AGGTCTTTGAGGGATTTGTAGTG G-3′ (antisense); for chemokine (C-C motif) ligand 2 (CCL2), 5′-AGCAGGT GTCCCAAAGAA-3′ (sense) and 5′-TATGTCTGGACCCATTCCTT-3′ (antisense); for CXCL10, 5′-GACGGTCCGCTGCAACTG-3′ (sense) and 5′-G CTTCCCTATGGCCCTCATT-3′ (antisense); for CXCL11, 5′-AAGCTCGCC TCATAATGCAG-3′ (sense) and 5′-CACAGTCAGACGTTCCCA-3′ (antisense); for CXCL12, 5′-CCAGAGCCAACGTCAAGCAT-3′ (sense) and 5′-C AGCCGTGCAACAATCTGAA-3′ (antisense); for CXCL13, 5′-CATAGATC GGATTCAAGTTACGCC-3′ (sense) and 5′-TCTTGGTCCAGATCACAACT TCA-3′ (antisense); for IL-21, 5′-GGACAGTATAGACGCTCACGAATG-3′ (sense) and 5′-CGTATCGTACTTCTCCACTTGCA-3′ (antisense); for APRIL (a proliferating-inducing ligand), 5′-TCCGATGTATCAGAAGTATGCC-3′ (sense) and 5′-CCCTTGATGTAAATGAAAGACACC-3′ (antisense); for B cell maturation protein antigen (BCMA), 5′-ATCTTCTTGGGGCTGACCT T-3′ (sense) and 5′-CTTTGAGGCTGGTCCTTCAG-3′ (antisense); for transmembrane activator and calcium modulator ligand interactor (TACI), 5′-GTG TGGCCACTTCTGTGAGA-3′ (sense) and 5′-CTGGTGCCTTCCTGAGTTG T-3′ (antisense); and for BAFF receptor (BAFF-R), 5′-CCCCAGACACTTCA GAAGGA-3′ (sense) and 5′-AGGTAGGAGCTGAGGCATGA-3′ (antisense). IFN-α4, IFN-β1, IFN-γ, and BAFF mRNA levels were determined using Applied Biosystems gene expression arrays with TaqMan fast universal PCR master mix (Applied Biosystems) in duplicate. PCR conditions were as follows: 20 s at 95°C, followed by 40 cycles, where 1 cycle consists of 3 s at 95°C and 30 s at 60°C. Transcript levels were calculated relative to the housekeeping gene GAPDH using the following formula: $2^{[C_T(\text{GAPDH}) - C_T(\text{target})]} \times 1{,}000$, where C_T is determined as the threshold cycle at which the fluorescent signal becomes significantly higher than that of the background and C_T (GAPDH) is the C_T for GAPDH.

Immunohistochemistry. Spinal cords were snap-frozen in Tissue-Tek optimum-cutting-temperature (OCT) compound, sectioned at 10 μm, fixed with 95% ethanol for 15 min at −20°C and permeabilized with acetone for 5 min at −20°C. The spinal cord sections were then blocked for 30 min and stained with either goat anti-BAFF (R&D Systems, Minneapolis, MN) and rabbit anti-glial fibrillary acidic protein (anti-GFAP) (Dako, Carpinteria, CA) or rabbit anti-APRIL (Abcam, Cambridge, MA) and rat anti-GFAP Ab (2.2B10; Invitrogen) overnight at 4°C. Rhodamine-labeled donkey anti-goat, Alexa Fluor 488-labeled goat anti-rabbit, Alexa Fluor 594-labeled goat anti-rabbit, and Alexa Fluor 488-labeled goat anti-rat (Invitrogen) Ab were added and left for 1 h. The sections were mounted with Vectashield mounting medium with 4′,6-diamidino-2-phenylindole (Vector Laboratories, Burlingame, CA). For BAFF immunoperoxidase staining, horse anti-goat secondary Ab and 3,3′-diaminobenzidine substrate (Vectastain-ABC kit; Vector Laboratories) were used.

Statistical analysis. Graphs were plotted and statistics were assessed using GraphPad Prism 3.0 software (La Jolla, CA). In all cases, a P of <0.05 was considered significant as determined by the unpaired t test.

RESULTS

T cell recruitment precedes ASC accumulation in the spinal cord. JHM virus (JHMV) replication is initiated in the brain following intracranial inoculation, but JHMV rapidly spreads to the spinal cord, where it preferentially establishes a persistent infection (6) (Fig. 1A). During viral persistence, enhanced immune activation in the spinal cord relative to the brain is indicated by higher frequencies of virus-specific $CD8^+$ T cells (38) as well as $CD138^+$ antibody-secreting cells (ASC) within the spinal cord (70). However, due to higher overall recovery of leukocytes from the brain compared to the spinal cord, the vast majority of kinetic and functional analysis of infiltrating cells is documented for the brain, where maximal lymphocyte accumulation occurs between days 7 and 9 p.i. (78). Thus, prior to analysis of ASC recruitment and survival factors, we established the relative kinetics of lymphocyte infiltration into the spinal cord (Fig. 1). Bone marrow-derived CNS infiltrating cells were distinguished from resident cells by a $CD45^{hi}$ phenotype. Similar to brain (6, 78), total $CD45^{hi}$ cell infiltrates, $CD4^+$ and $CD8^+$ T cells peaked prior to day 14 p.i. (Fig. 1B and C). Although $CD19^+$ B cells were present at day 7 p.i.,

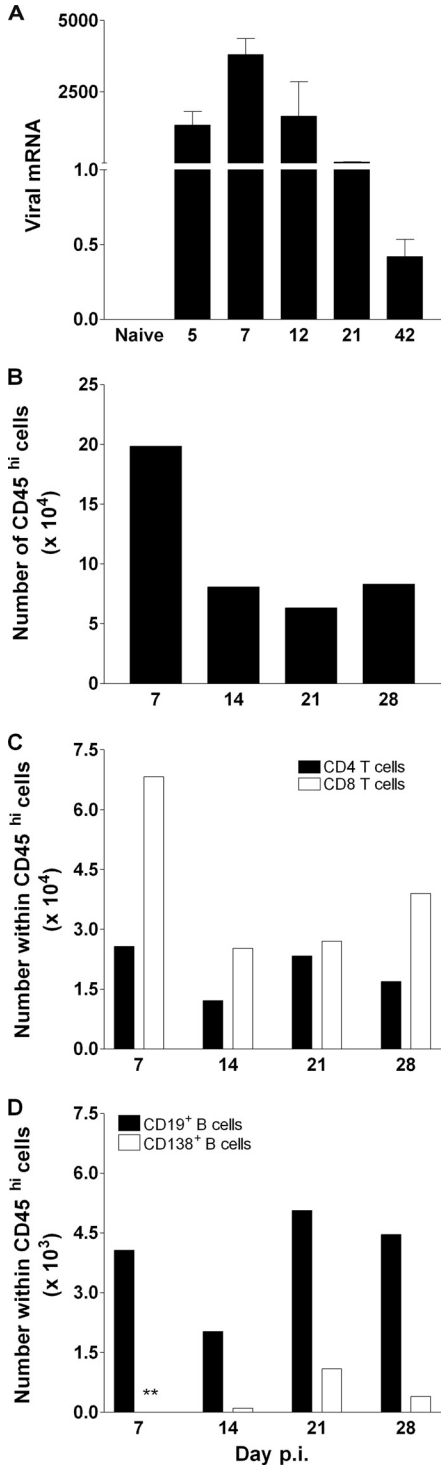

FIG. 1. Different kinetics of T cell and ASC recruitment into the CNS. (A) Viral mRNA in spinal cords relative to GAPDH values. The values are means plus standard errors of the means (SEM) (error bars). Data are derived from 3 or 4 individual mice and are representative of 2 separate experiments. (B to D) Cells isolated from pooled spinal cords of infected wt mice ($n = 3$ or 4) analyzed for CD45, CD4, CD8, CD19, and CD138 expression by flow cytometry. (B) Total numbers of bone marrow-derived $CD45^{hi}$ CNS-infiltrating cells per spinal cord. (C and D) Numbers of $CD4^+$ and $CD8^+$ T cells (C) or $CD19^+$ B cells and $CD138^+$ B cells (D) within the infiltrating $CD45^{hi}$ population. Data are representative of three independent experiments. Levels below detection are indicated (**).

their numbers were lower than the numbers of T cells and remained relatively constant through day 28 p.i. (Fig. 1D). However, the vast majority of $CD19^+$ B cells do not express CD138 which characterizes ASC (1). $CD138^+$ ASC did not accumulate until day 21 p.i. (Fig. 1D), similar to their delayed migration to the brain subsequent to clearance of infectious virus (57, 70).

Relative kinetics of ASC infiltration and chemokine expression in the CNS. Migration of lymphocytes into inflamed tissues is guided by chemokines, predominantly the CXCR3 ligands CXCL9, CXCL10, and CXCL11 as well as the chemokine (C-C motif) receptor 5 (CCR5) ligands CCL3, CCL4, and CCL5 (11). Although these chemokines function as T cell attractants during various infections, including JHMV (70), recruitment signals for ASC into inflamed tissues are less well defined. CXCR3 ligands CXCL9, CXCL10, and CXCL11 mediate plasmablast migration *in vitro* (20), while CXCL12 is critical for ASC homing to the bone marrow (14). CXCL13 expression within lymphoid tissue guides B cell entry into B cell zones (2) and is associated with ectopic lymphoid structures in the CNS (13, 36, 64). In addition to the spinal cord, chemokine mRNA expression was assessed in the draining cervical lymph nodes (CLN) to gauge relative levels as well as alterations in the periphery. Notably, following JHMV infection, both T and B cells are primed in CLN with little evidence for productive viral infection (39). As expected, naive levels of all chemokines in the CLN exceeded those in the CNS (Fig. 2). At day 5 p.i., CXCL9, CXCL10, and CXCL11 mRNA levels in CLN were enhanced only 2- to 3-fold and rapidly returned to baseline by day 7 p.i. This contrasts with the >800-fold induction of CXCL9, CXCL10, and CXCL11 in the CNS, where these CXCR3 ligands were significantly elevated by day 5 p.i. and reached peak levels by day 7 p.i. (Fig. 2A), coincident with initial T cell infiltration (Fig. 1C). Although maximal mRNA expression of CXCL9 in the CNS did not reach CLN levels, CXCL10 and CXCL11 mRNA levels in the CNS exceeded the CLN levels, suggesting potent migration signals. CXCL9, CXCL10, and CXCL11 mRNA levels all declined by day 12 p.i. in the CNS but were still significantly elevated through day 42 p.i. (Fig. 2A). Of note, CXCL9 mRNA levels underwent the slowest relative decline implicating CXCL9 as a sustained lymphocyte recruitment factor. Although the CXCL11 gene does not give rise to a functional protein in C57BL/6 mice (46), it was included to survey transcriptional regulation. Similar to the CXCR3 ligands, CXCL12 and CXCL13 mRNA in the naive CLN exceeded the levels in the naive CNS; however, expression was not upregulated following infection (Fig. 2B). Indeed, CXCL12 expression decreased, consistent with the downregulation of other chemokines in the spleen and lymph nodes following systemic viral infection (45). CXCL12 mRNA levels in the CNS remained comparable to naive mice with only a slight increase at day 42 p.i. Although induction of CXCL13 mRNA in the CNS resembled induction of CXCL9, CXCL10, and CXCL11, with peak expression at day 7 p.i. and a subsequent decline, expression remained several orders of magnitude lower than in the CLN. Nevertheless, the possibility that CXCL13-expressing CNS-infiltrating dendritic cells may contribute to local B cell activation or differentiation as implied in CNS autoimmunity cannot be excluded (36, 63, 64). These data indicate that infection of the spinal cord leads to the induction

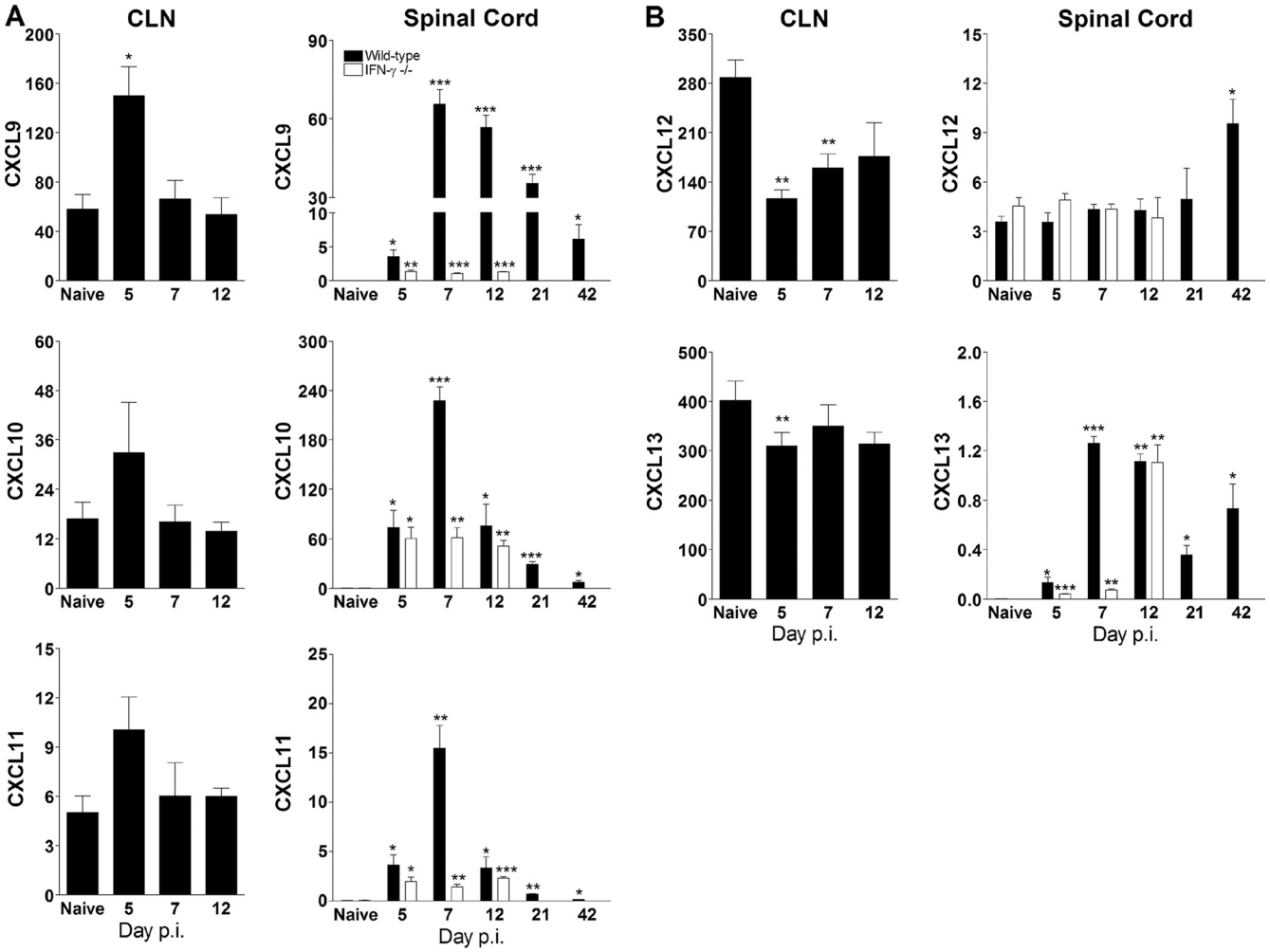

FIG. 2. Sustained mRNA expression of B cell homing chemokines during ASC recruitment. Levels of CXCL9, CXCL10, CXCL11 mRNA (A) and CXCL12 and CXCL13 mRNA (B) in CLN and spinal cords of naive and infected mice. Wild-type mice (black bars) and IFN-$\gamma^{-/-}$ mice (white bars) were used. Data are representative of two independent experiments and are expressed as means plus SEM (error bars) relative to GAPDH values. Statistically significant differences between the values for samples from naive and infected mice are indicated as follows: *, $P < 0.05$; **, $P < 0.005$; ***, $P < 0.001$.

of chemokine expression, of which CXCL9 is most prominently sustained throughout persistence. These data suggest that CXCR3 ligands, but not CXCL12, are likely candidates contributing to ASC recruitment in response to CNS infection.

CXCL10 and CXCL11 transcription is induced by innate IFN-α/β as well as IFN-γ (12, 32). In contrast, CXCL9 induction is IFN-γ dependent (16), predominantly derived from CNS-infiltrating T cells during JHMV infection (78). To assess how the relative chemokine expression patterns correlate with IFN expression, IFN-α/β and IFN-γ mRNA were analyzed longitudinally. Both IFN-α4 and IFN-β1 mRNA peaked prior to IFN-γ as expected (Table 1). IFN-α4 and IFN-β1 were readily detectable at day 5 p.i., declined significantly by day 7 p.i., and remained slightly elevated above background through 21 p.i. (Table 1). In contrast, IFN-γ levels were low at day 5 p.i. and maximal by day 7 p.i. and dropped gradually thereafter, consistent with T cell effector function (Table 1). Overall, the early increase in CXCL10 and CXCL11 expres-

TABLE 1. Differential expression of IFNs in the CNS

Gene	Relative transcript level (mean ± SEM)[a]					
	Naive mice	Day 5 p.i.	Day 7 p.i.	Day 12 p.i.	Day 21 p.i.	Day 42 p.i.
IFN-α4	0.0004 ± 0.00005	0.2 ± 0.08	0.04 ± 0.01	0.003 ± 0.002	0.005 ± 0003	0.001 ± 0.0004
IFN-β1	0.003 ± 0.0008	1.9 ± 0.6	0.4 ± 0.1	0.09 ± 0.7	0.04 ± 0.02	0.004 ± 0.002
IFN-γ	0.003 ± 0.0006	0.1 ± 0.04	3.2 ± 0.8	0.8 ± 0.1	0.4 ± 0.07	0.04 ± 0.01

[a] Relative transcript levels normalized to GAPDH values. The data are from 3 or 4 individual spinal cords.

sion was consistent with IFN-α/β induction, whereas the temporally delayed, but more sustained CXCL9 expression reflected the kinetics and magnitude of IFN-γ expression. This was confirmed by chemokine expression in JHMV-infected IFN-γ-deficient (IFN-$\gamma^{-/-}$) mice (Fig. 2). Analysis of IFN-$\gamma^{-/-}$ mice was limited to 2 weeks p.i., as the majority succumb to infection between 12 and 21 days p.i. (52). Induction of CXCL9 was significantly lower in the CNS of IFN-$\gamma^{-/-}$ mice between days 5 and 12 p.i., whereas the levels of CXCL10 and CXCL11 transcripts were similar to those of wt mice at day 5 p.i. (Fig. 2A). However, while peak IFN-γ levels were reflected in increased CXCL10 and CXCL11 upregulation in wt mice at day 7 p.i., both chemokine mRNA levels remained low until day 12 p.i. Finally, the absence of IFN-γ did not affect CXCL12 expression; however, CXCL13 induction was markedly decreased in the absence of IFN-γ (Fig. 2B).

CNS expression of B cell differentiation and survival factors. Delayed accumulation of $CD138^+$ ASC in the CNS relative to both T cells and $CD19^+$ $CD138^-$ B cells suggests that $CD19^+$ B cells may differentiate at the site of infection. Differentiation *in situ* is supported by the gradual loss of MHC class II on $CD138^+$ plasmablasts in the CNS during persistent infection (70), implying local CNS expression of B cell differentiation factors. A key cytokine implicated in B cell proliferation/differentiation is IL-21, which is predominantly secreted by $CD4^+$ T cells (28) and drives the generation of follicular helper $CD4^+$ T cells and thus germinal center formation (31, 73, 77). Following JHMV infection, IL-21 mRNA in CLN was upregulated ~3-fold by day 5 p.i. and sustained at least until day 12 p.i. (Fig. 3A), when virus-specific ASC frequencies peak in the periphery (70). IL-21 transcripts were also increased in the spinal cord of infected mice at day 7 p.i., coincident with initial $CD4^+$ T cell infiltration (Fig. 1C), and remained elevated through day 21 p.i. (Fig. 3B). Indeed, expression of IL-21 mRNA was considerably higher in purified CNS-infiltrating $CD4^+$ T cells versus $CD8^+$ T cells or resident $CD45^{lo}$ microglia (Fig. 3C). Furthermore, IL-21 expression in the CNS was independent of IFN-γ (Fig. 3B).

In addition to IL-21, APRIL, BAFF, and IL-6 are critical for B cell differentiation and survival (3, 4, 8, 10, 40, 47, 60, 61). IL-6, APRIL, and BAFF are predominantly expressed by monocytes, macrophages, and dendritic cells in the periphery (34, 41). However, IL-6 in the CNS is produced primarily by astrocytes (72), which also produce both APRIL and BAFF *in vivo* (27, 68). Nevertheless, microglia also produce IL-6 (29, 74) and BAFF *in vitro* (24). Similar to the chemokines, BAFF and APRIL mRNA were constitutively expressed at high levels in the CLN, and no further induction was noted in response to infection (Fig. 4A). IL-6 transcripts in the CNS were readily detectable at day 5 p.i. and declined to near basal levels a week later (Fig. 4B). Not surprising, the absence of IFN-γ had no significant effect on IL-6 mRNA expression in the CNS (Fig. 4B). BAFF mRNA was constitutively expressed in the CNS, but levels increased by 2- to 3-fold through days 7 to 21 p.i. consistent with IFN-γ-mediated regulation (Fig. 4B). In contrast to the modest BAFF induction, APRIL transcripts were upregulated ~20-fold by day 12 p.i. and were sustained until at least day 21 p.i. Of note, peak expression of both APRIL and BAFF transcripts in the CNS approached basal levels in the CLN (Fig. 4), but was delayed relative to chemokine mRNAs

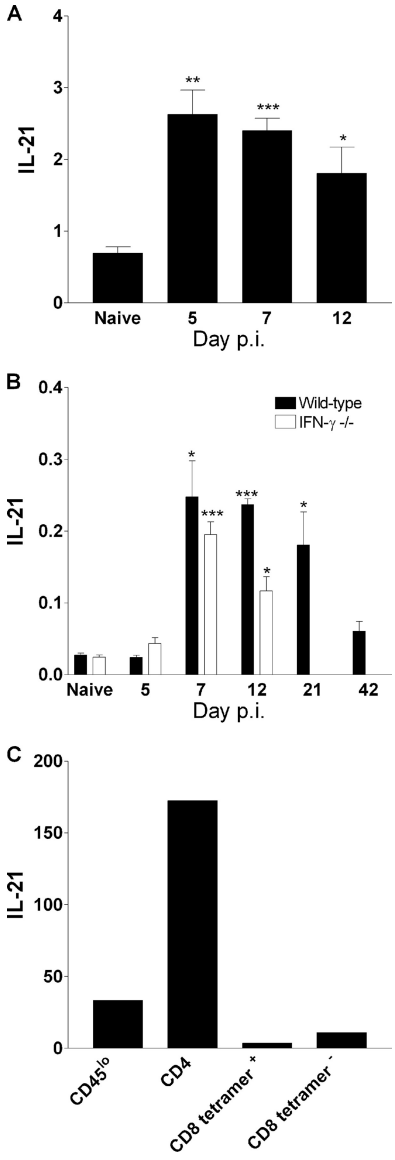

FIG. 3. IL-21 expression in the CNS during infection. (A) IL-21 mRNA in the CLN of naive and infected wt mice. (B) IL-21 mRNA in the spinal cords of infected wt and IFN-$\gamma^{-/-}$ mice ($n = 3$ or 4). Data are representative of two independent experiments and are expressed as means plus SEM (error bars) relative to GAPDH values. (C) IL-21 mRNA expression in purified $CD45^{lo}$ microglia, $CD4^+$ T cells, and tetramer-positive (tetramer$^+$) and tetramer-negative (tetramer$^-$) $CD8^+$ T cells from pooled wt brains 7 days p.i. Statistically significant differences between the values for samples from naive and infected mice are indicated as follows: *, $P < 0.05$; **, $P < 0.005$; ***, $P < 0.001$.

(Fig. 2). IFN-γ deficiency did not alter the basal levels of BAFF mRNA in the spinal cord (Fig. 4B); however, the increase of BAFF transcripts at day 7 p.i. was abrogated, supporting BAFF induction by IFN-γ (27). In contrast, APRIL induction was IFN-γ independent and followed the same delayed kinetics as in wt mice (Fig. 4B), indicating distinct regulation of BAFF and APRIL in the CNS.

To identify the cellular source of APRIL and BAFF, microglia, an astrocyte-enriched population, and infiltrating monocyte-derived macrophages were purified at 10 days p.i. The

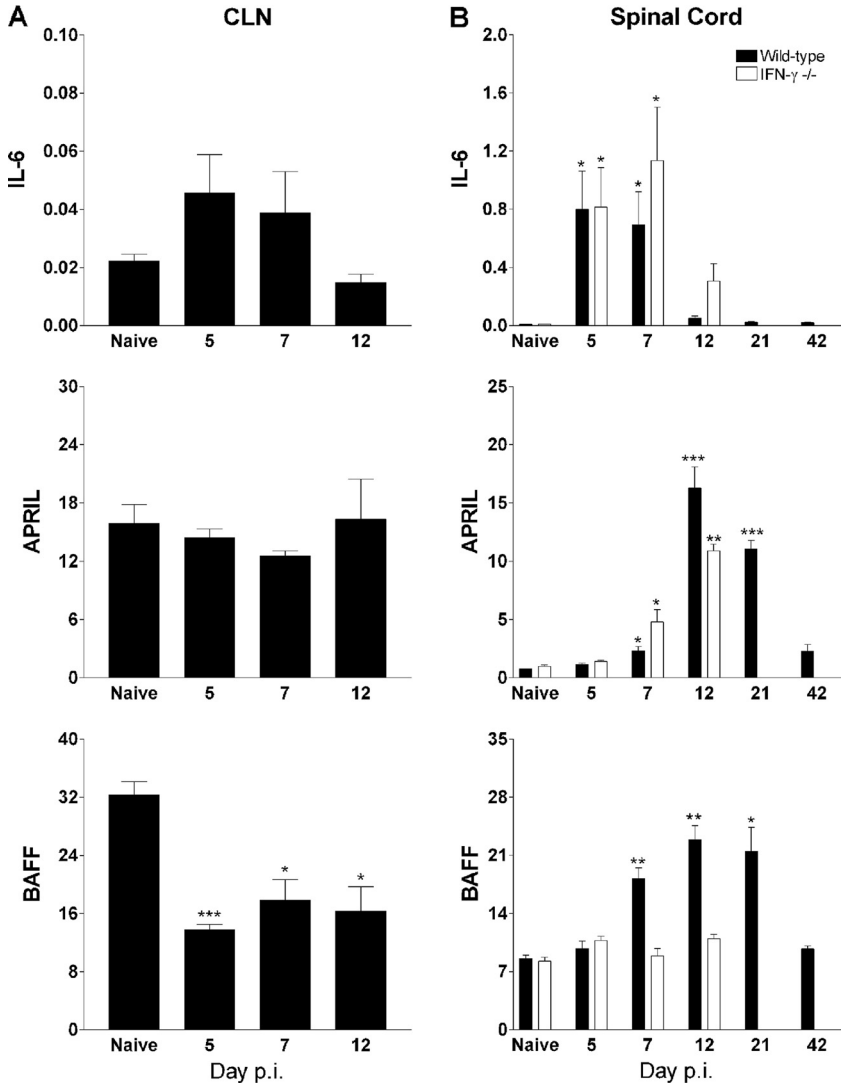

FIG. 4. The levels of expression of APRIL and BAFF are maintained throughout ASC accumulation. (A) IL-6, APRIL, and BAFF mRNA in the CLN of naive and infected wt mice ($n = 3$ or 4). (B) IL-6, APRIL, and BAFF mRNA in the spinal cords of naive or infected wt and IFN-$\gamma^{-/-}$ mice ($n = 3$ or 4). Data are representative of two independent experiments and are expressed as the means plus SEM (error bars) relative to GAPDH values. Statistically significant differences between the values for samples from naive and infected mice are indicated as follows: *, $P < 0.05$; **, $P < 0.005$; ***, $P < 0.001$.

levels of expression of APRIL and BAFF mRNA by astrocytes were increased ~80- and 5-fold, respectively (Table 2). In microglia, APRIL transcripts were enhanced ~9-fold, while BAFF expression was not altered (Table 2). Modest changes were also detected in infiltrating monocyte-derived macrophages with 1.5- and 2.1-fold increases in APRIL and BAFF, respectively (Table 2). These data suggest that astrocytes are likely the primary source of BAFF and APRIL during JHMV infection, with microglia making an additional minor contribution to APRIL expression. Immunohistochemical analysis revealed BAFF expression in parenchymal cells consistent with astrocyte morphology at day 14 p.i. (Fig. 5A). Dual staining confirmed that astrocytes are the predominant BAFF producers, although only a minority expressed BAFF (Fig. 5B). Astrocytes were also the prominent cell type producing APRIL (Fig. 5C). Interestingly, in contrast to the cytoplasmic distribution of BAFF, APRIL localized primarily to astrocyte processes. Sustained elevated expression of IL-21, APRIL, and BAFF thus support the notion that persisting CNS infection provides a local niche capable of supporting ASC survival.

TABLE 2. APRIL and BAFF expression in purified cell populations

Gene	Fold increase (mean ± SEM)[a] in:		
	Astrocytes	Microglia	Monocyte-derived macrophages
APRIL	79.3 ± 6.5	8.5 ± 0.3	1.5 ± 0.03
BAFF	5.3 ± 0.2	0.9 ± 0.02	2.1 ± 0.2

[a] APRIL and BAFF transcript levels relative to GAPDH values are presented as fold increases with the APRIL and BAFF transcript levels from samples from naïve mice set at 1. APRIL and BAFF transcript levels were taken on day 10 p.i.

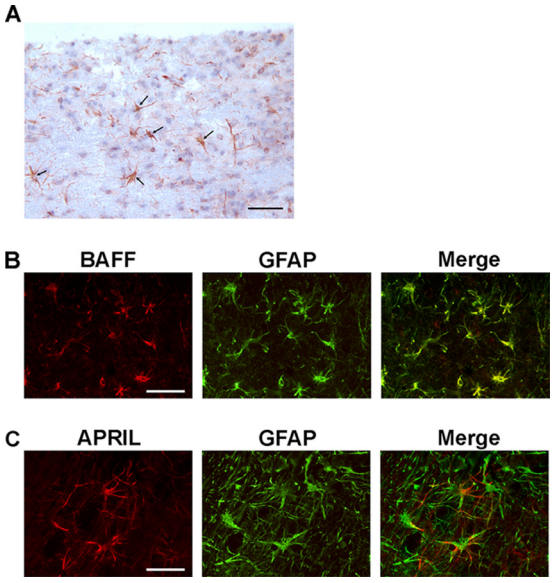

FIG. 5. Astrocytes express APRIL and BAFF. (A) Immunoperoxidase stain using anti-BAFF Ab with hematoxylin counterstain. Cells expressing BAFF are indicated by the small black arrows. Bar, 50 μm. (B and C) BAFF and APRIL localization in spinal cords from JHMV-infected mice identified by their respective Ab. Astrocytes were visualized with anti-GFAP Ab. Merged images of APRIL or BAFF with GFAP image are shown. Bars, 50 μm.

BCMA and TACI expression coincides with ASC accumulation. APRIL and BAFF exert their functions by signaling through receptors expressed differentially in distinct B cell subsets (8, 33, 37, 47). While both APRIL and BAFF bind B cell maturation antigen (BCMA) and transmembrane activator and calcium modulator ligand interactor (TACI), BAFF additionally binds to BAFF receptor (BAFF-R). Signaling through BAFF-R plays a fundamental role in the transition from immature B cells to mature B cells (34, 66), as well as promoting survival and maintenance of mature B cells (59). TACI functions to support survival of activated plasmablasts (8) and promote plasma cell differentiation (37). Similarly, BCMA expression is primarily limited to plasma cells and plays a critical role in survival (4, 47). The low frequency of ASC within the CNS precluded direct analysis of receptor expression on purified populations. Thus, expression of receptor mRNA was initially assessed in purified splenic B cells ($CD19^+$ $CD138^-$ IgD^+ GFP^-) and ASC ($CD19^{dim}$ $CD138^+$ IgD^- GFP^+) from both naive and JHMV-immunized Blimp-1-$GFP^{+/-}$ mice to verify differential expression. The majority of B cells in the spleen were of an immature phenotype, regardless of immunization (89% ± 3% for naive mice and 81% ± 1.5% for immunized mice). However, following immunization, ASC increased from 0.6% ± 0.2% in naive mice to 3.1% ± 0.1% by day 7 postimmunization. Naive B cells expressed higher levels of BAFF-R mRNA than the ASC population. TACI mRNA was detected in both naive B cells and ASC but was increased ~2-fold in the latter. BCMA transcripts were exclusively expressed by ASC and not naive B cells, independent of immunization (Fig. 6A), confirming previous studies (4). BCMA expression was thus used as a reliable marker specifically for ASC accumulation within the CNS. Expression of BAFF-R mRNA in spinal cords remained near naive levels throughout infection (Fig. 6B), suggesting no role in CNS B cell homeostasis during JHMV infection. Importantly, neither BCMA nor TACI transcripts were significantly increased until day 21 p.i. (Fig. 6B), corresponding to peak $CD19^+$ $CD138^+$ ASC infiltration (Fig. 1D). Furthermore, BCMA transcripts were sustained throughout day 42 p.i., while TACI mRNA decreased slightly. Overall, detection of BCMA and TACI mRNA concurred with ASC recruitment and retention, suggesting that APRIL and BAFF contribute to sustained ASC survival within the CNS.

DISCUSSION

Accumulation and retention of virus-specific ASC within the CNS are hallmarks of many neurotropic viral infections, including rabies virus (22), measles virus (9, 48), Theiler's murine encephalomyelitis virus (50, 51), Semliki Forest virus (43), and Sindbis virus (71) infections. In general, viral infections induce both short- and long-lived ASC with the latter emerging after germinal center selection (35, 44). A proportion of ASC surviving germinal center selection migrate to the bone marrow via CXCR4-driven signals, where they undergo terminal differentiation and subsequently lose their capacity to migrate (65). In the bone marrow, stromal cells, myeloid cells, and megakaryocytes constitutively secrete B cell survival factors (3, 44, 75), providing a survival niche for fully differentiated long-lived ASC. Bone marrow ASC are the primary source of protective antiviral Ab. In contrast, neither the factors underlying recruitment or differentiation into mature plasma cells nor the expression of ASC survival factors in the CNS have been characterized.

High steady-state expression of transcripts in the CLN compared to the CNS in naive mice is consistent with normal homeostasis of the B cell compartment. In contrast to bone marrow, the CNS expresses negligible levels of factors promoting ASC recruitment and survival. Although CXCL12 is expressed constitutively in the CNS, similar to bone marrow (7), other ASC chemoattractants, i.e., CXCL9, CXCL10, CXCL11, or the B cell chemoattractant CXCL13, are barely detectable in the absence of inflammation. With the exception of CXCL12, the expression of all chemokines peaked coincident with recruitment of inflammatory cells. Although expression of the IFN-γ-dependent CXCR3 binding chemokines decrease as infectious virus is controlled (52) and the inflammatory response resolves, they remained significantly elevated during the appearance of ASC in the CNS, particularly CXCL9. The increase in CXCL12 during persistent infection suggested an additional function of this chemokine as both a recruiting (15, 19) and survival factor (10), similar to its role in bone marrow. Last, although CXCL13 does not act on ASC recruitment (20), the possibility that CNS-infiltrating, CXCL13-expressing dendritic cells contribute to recruitment of newly primed B cells into the CNS cannot be excluded.

The possibility that naive, or recently primed B cells, are recruited into the CNS and subsequently undergo differentiation *in situ* is supported by the formation of lymphoid follicle-like structures during chronic autoimmune inflammation (36, 63, 64). However, lymphoid follicles have not been reported during virus-induced CNS inflammation (43, 56), including

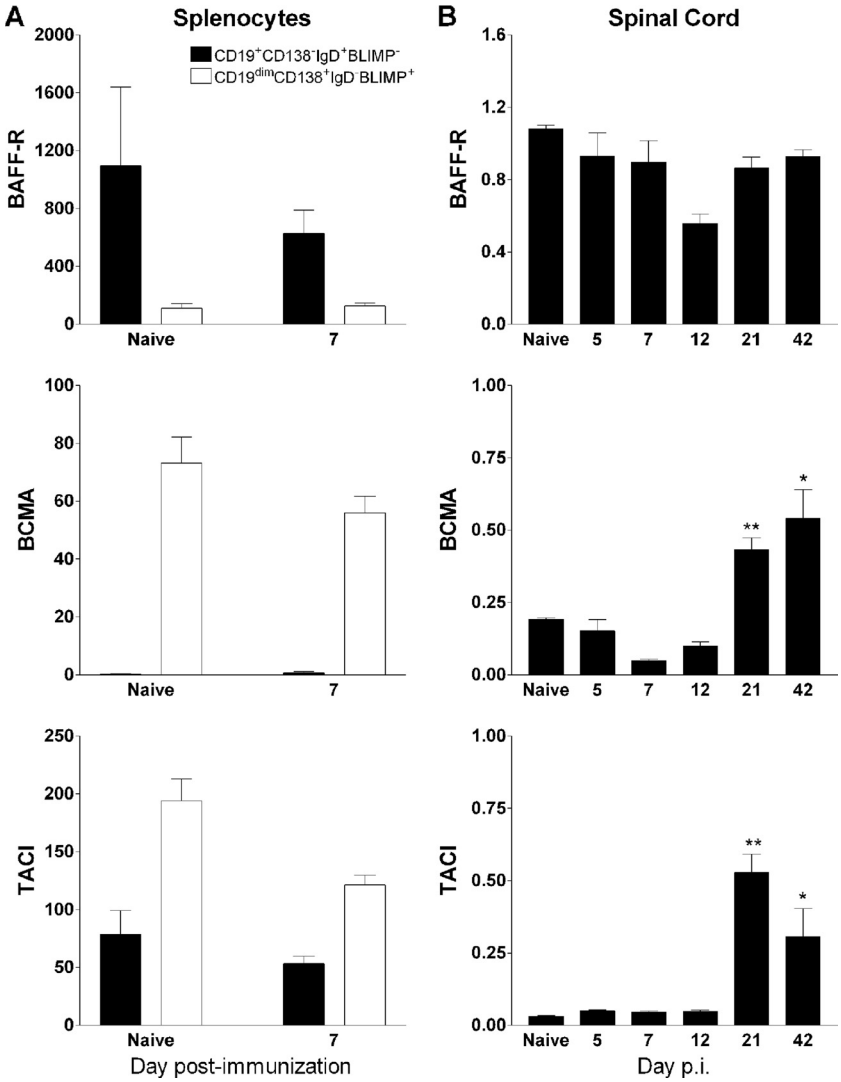

FIG. 6. BCMA and TACI expression coincides with ASC infiltration into the CNS. (A) BCMA, TACI, and BAFF-R mRNA expression in purified immature B cells ($CD19^+$ $CD138^-$ IgD^+ GFP^-) or ASC ($CD19^{dim}$ $CD138^+$ IgD^- GFP^+) from pooled spleen cells from naive or JHMV-immunized mice ($n = 2$ or 3). (B) BCMA, TACI, and BAFF-R mRNA expression in the spinal cords of naive or infected wt mice ($n = 3$ or 4). Data are representative of two independent experiments and are expressed as the means plus SEM (error bars) relative to GAPDH values. Statistically significant differences between the values for samples from naive and infected mice are indicated as follows: *, $P < 0.05$; **, $P < 0.005$.

JHMV encephalomyelitis (data not show). Nevertheless, ongoing differentiation of ASC into terminally differentiated sessile plasma cells is suggested by the gradual MHC class II downregulation during persistent JHMV infection (70). The factors promoting ASC differentiation within the CNS may include both CXCL13 and IL-21. In germinal center responses, IL-21 is primarily secreted by $CD4^+$ T follicular helper cells (67) and acts directly on B cells to promote differentiation and survival (26) as well as Ab production (49). IL-21 mRNA was increased and sustained in the CLN following JHMV infection, supporting a contribution of IL-21 to the differentiation of B and T cells. This observation is also consistent with increased IL-21 expression in the spleens of mice infected with lymphocytic choriomeningitis virus or herpes simplex virus (21). Supporting the absence of a correlation between IL-21 and IFN-γ mRNAs in herpes simplex virus-infected mice (21), IL-21 expression was also IFN-γ independent in the CNS. Our data are the first to show recruitment of IL-21-expressing $CD4^+$ T cells into the CNS, thus indicating their potential to support both B cell differentiation and $CD8^+$ T cell function locally.

Immunohistochemical identification of ASC, as well as their isolation and functional characterization, indicated that the CNS provides long-term survival signals during viral persistence (69, 70). This notion was supported by the induction of BAFF and APRIL, both prominent ASC survival factors in bone marrow, during JHMV encephalomyelitis. BAFF upregulation was IFN-γ dependent and coincident with the inflammatory response; however, expression was not sustained above basal levels during persistence. In contrast, the delayed induction of APRIL did not coincide with IFN-γ or other proinflammatory factors. Immunohistochemical analysis implicated astrocytes as a primary source of both BAFF and APRIL

during JHMV infection, although increased APRIL mRNA expression was also found in microglia and infiltrating monocyte-derived macrophages. The distinct localization of APRIL and BAFF may reside in the differential processing of these cytokines. While BAFF is cleaved from the cell membrane, APRIL is cleaved in the Golgi apparatus and thus directly transported intracellularly as a trimeric active form (25, 42). In addition, concentrated APRIL staining localized to astrocyte processes may reflect binding to dense areas of heparan sulfate proteoglycan deposition (25), which may serve to enhance signaling in target cells. The observations that infiltrating monocyte-derived macrophages are most prominent early during infection and decline significantly by day 14 p.i. (62) argue that cells from this lineage do not contribute significantly to sustained ASC survival within the CNS. Expression of APRIL and BAFF precedes ASC recruitment into the CNS; however, expression of their receptors, BCMA and TACI, corresponds exclusively to ASC recruitment. Moreover, use of the ratio of BCMA to TACI expression as an indicator of ASC maturation reveals that the BCMA/TACI ratio remains consistent at ~0.4 in splenic ASC; however, in the CNS, the ratio increases from 0.6 to 1.8 during viral persistence, supporting preferential maintenance and/or survival of more differentiated ASC within the CNS, already indicated by progressive downregulation of MHC class II expression (70).

In summary, our data demonstrate induction of critical factors associated with ASC migration, differentiation, and survival during acute viral encephalomyelitis, prior to ASC accumulation in the CNS. The rapid establishment and prolonged maintenance of an environment capable of supporting B cell differentiation and ASC survival thus guarantee survival of plasmablasts emigrating from lymphoid organs and their subsequent differentiation into locally protective antiviral ASC.

ACKNOWLEDGMENTS

This work was supported by U.S. National Institutes of Health grant AI 47249.

We sincerely thank Wenqiang Wei for exceptional technical assistance.

REFERENCES

1. **Angelin-Duclos, C., G. Cattoretti, K. I. Lin, and K. Calame.** 2000. Commitment of B lymphocytes to a plasma cell fate is associated with Blimp-1 expression in vivo. J. Immunol. **165:**5462–5471.
2. **Ansel, K. M., et al.** 2000. A chemokine-driven positive feedback loop organizes lymphoid follicles. Nature **406:**309–314.
3. **Belnoue, E., et al.** 2008. APRIL is critical for plasmablast survival in the bone marrow and poorly expressed by early-life bone marrow stromal cells. Blood **111:**2755–2764.
4. **Benson, M. J., et al.** 2008. The dependence of plasma cells and independence of memory B cells on BAFF and APRIL. J. Immunol. **180:**3655–3659.
5. **Bergmann, C. C., J. D. Altman, D. Hinton, and S. A. Stohlman.** 1999. Inverted immunodominance and impaired cytolytic function of CD8+ T cells during viral persistence in the central nervous system. J. Immunol. **163:**3379–3387.
6. **Bergmann, C. C., T. E. Lane, and S. A. Stohlman.** 2006. Coronavirus infection of the central nervous system: host-virus stand-off. Nat. Rev. Microbiol. **4:**121–132.
7. **Bleul, C. C., R. C. Fuhlbrigge, J. M. Casasnovas, A. Aiuti, and T. A. Springer.** 1996. A highly efficacious lymphocyte chemoattractant, stromal cell-derived factor 1 (SDF-1). J. Exp. Med. **184:**1101–1109.
8. **Bossen, C., et al.** 2008. TACI, unlike BAFF-R, is solely activated by oligomeric BAFF and APRIL to support survival of activated B cells and plasmablasts. Blood **111:**1004–1012.
9. **Burgoon, M. P., et al.** 2005. Laser-capture microdissection of plasma cells from subacute sclerosing panencephalitis brain reveals intrathecal disease-relevant antibodies. Proc. Natl. Acad. Sci. U. S. A. **102:**7245–7250.
10. **Cassese, G., et al.** 2003. Plasma cell survival is mediated by synergistic effects of cytokines and adhesion-dependent signals. J. Immunol. **171:**1684–1690.
11. **Charo, I. F., and R. M. Ransohoff.** 2006. The many roles of chemokines and chemokine receptors in inflammation. N. Engl. J. Med. **354:**610–621.
12. **Cole, K. E., et al.** 1998. Interferon-inducible T cell alpha chemoattractant (I-TAC): a novel non-ELR CXC chemokine with potent activity on activated T cells through selective high affinity binding to CXCR3. J. Exp. Med. **187:**2009–2021.
13. **Corcione, A., et al.** 2004. Recapitulation of B cell differentiation in the central nervous system of patients with multiple sclerosis. Proc. Natl. Acad. Sci. U. S. A. **101:**11064–11069.
14. **Cyster, J. G.** 2003. Homing of antibody secreting cells. Immunol. Rev. **194:**48–60.
15. **Cyster, J. G., K. M. Ansel, V. N. Ngo, D. C. Hargreaves, and T. T. Lu.** 2002. Traffic patterns of B cells and plasma cells. Adv. Exp. Med. Biol. **512:**35–41.
16. **Farber, J. M.** 1990. A macrophage mRNA selectively induced by gamma-interferon encodes a member of the platelet factor 4 family of cytokines. Proc. Natl. Acad. Sci. U. S. A. **87:**5238–5242.
17. **Griffin, D. E.** 2003. Immune responses to RNA-virus infections of the CNS. Nat. Rev. Immunol. **3:**493–502.
18. **Griffin, D. E.** 1981. Immunoglobulins in the cerebrospinal fluid: changes during acute viral encephalitis in mice. J. Immunol. **126:**27–31.
19. **Hargreaves, D. C., et al.** 2001. A coordinated change in chemokine responsiveness guides plasma cell movements. J. Exp. Med. **194:**45–56.
20. **Hauser, A. E., et al.** 2002. Chemotactic responsiveness toward ligands for CXCR3 and CXCR4 is regulated on plasma blasts during the time course of a memory immune response. J. Immunol. **169:**1277–1282.
21. **Holm, C., C. G. Nyvold, S. R. Paludan, A. R. Thomsen, and M. Hokland.** 2006. Interleukin-21 mRNA expression during virus infections. Cytokine **33:**41–45.
22. **Hooper, D. C., T. W. Phares, M. J. Fabis, and A. Roy.** 2009. The production of antibody by invading B cells is required for the clearance of rabies virus from the central nervous system. PLoS Negl. Trop. Dis. **3:**e535.
23. **Ireland, D. D., et al.** 2009. RNase L mediated protection from virus induced demyelination. PLoS Pathog. **5:**e1000602.
24. **Kim, K. S., J. Y. Park, I. Jou, and S. M. Park.** 2009. Functional implication of BAFF synthesis and release in gangliosides-stimulated microglia. J. Leukoc. Biol. **86:**349–359.
25. **Kimberley, F. C., J. P. Medema, and M. Hahne.** 2009. APRIL in B-cell malignancies and autoimmunity. Results Probl. Cell Differ. **49:**161–182.
26. **Konforte, D., N. Simard, and C. J. Paige.** 2009. IL-21: an executor of B cell fate. J. Immunol. **182:**1781–1787.
27. **Krumbholz, M., et al.** 2005. BAFF is produced by astrocytes and up-regulated in multiple sclerosis lesions and primary central nervous system lymphoma. J. Exp. Med. **201:**195–200.
28. **Leonard, W. J., and R. Spolski.** 2005. Interleukin-21: a modulator of lymphoid proliferation, apoptosis and differentiation. Nat. Rev. Immunol. **5:**688–698.
29. **Lin, H. Y., et al.** 13 October 2010. Peptidoglycan induces interleukin-6 expression through the TLR2 receptor, JNK, c-Jun and AP-1 pathways in microglia. J. Cell. Physiol. doi:10.1002/jcp.22489. [Epub ahead of print.]
30. **Lin, M. T., D. R. Hinton, N. W. Marten, C. C. Bergmann, and S. A. Stohlman.** 1999. Antibody prevents virus reactivation within the central nervous system. J. Immunol. **162:**7358–7368.
31. **Linterman, M. A., et al.** 2010. IL-21 acts directly on B cells to regulate Bcl-6 expression and germinal center responses. J. Exp. Med. **207:**353–363.
32. **Luster, A. D., and J. V. Ravetch.** 1987. Biochemical characterization of a gamma interferon-inducible cytokine (IP-10). J. Exp. Med. **166:**1084–1097.
33. **Mackay, F., and P. Schneider.** 2008. TACI, an enigmatic BAFF/APRIL receptor, with new unappreciated biochemical and biological properties. Cytokine Growth Factor Rev. **19:**263–276.
34. **Mackay, F., P. Schneider, P. Rennert, and J. Browning.** 2003. BAFF and APRIL: a tutorial on B cell survival. Annu. Rev. Immunol. **21:**231–264.
35. **MacLennan, I. C., et al.** 2003. Extrafollicular antibody responses. Immunol. Rev. **194:**8–18.
36. **Magliozzi, R., S. Columba-Cabezas, B. Serafini, and F. Aloisi.** 2004. Intracerebral expression of CXCL13 and BAFF is accompanied by formation of lymphoid follicle-like structures in the meninges of mice with relapsing experimental autoimmune encephalomyelitis. J. Neuroimmunol. **148:**11–23.
37. **Mantchev, G. T., C. S. Cortesao, M. Rebrovich, M. Cascalho, and R. J. Bram.** 2007. TACI is required for efficient plasma cell differentiation in response to T-independent type 2 antigens. J. Immunol. **179:**2282–2288.
38. **Marten, N. W., S. A. Stohlman, and C. C. Bergmann.** 2000. Role of viral persistence in retaining $CD8^+$ T cells within the central nervous system. J. Virol. **74:**7903–7910.
39. **Marten, N. W., S. A. Stohlman, J. Zhou, and C. C. Bergmann.** 2003. Kinetics of virus-specific $CD8^+$-T-cell expansion and trafficking following central nervous system infection. J. Virol. **77:**2775–2778.
40. **Minges Wols, H. A., G. H. Underhill, G. S. Kansas, and P. L. Witte.** 2002. The role of bone marrow-derived stromal cells in the maintenance of plasma cell longevity. J. Immunol. **169:**4213–4221.
41. **Mohr, E., et al.** 2009. Dendritic cells and monocyte/macrophages that create

the IL-6/APRIL-rich lymph node microenvironments where plasmablasts mature. J. Immunol. **182:**2113–2123.
42. **Moisini, I., and A. Davidson.** 2009. BAFF: a local and systemic target in autoimmune diseases. Clin. Exp. Immunol. **158:**155–163.
43. **Mokhtarian, F., C. M. Huan, C. Roman, and C. S. Raine.** 2003. Semliki Forest virus-induced demyelination and remyelination–involvement of B cells and anti-myelin antibodies. J. Neuroimmunol. **137:**19–31.
44. **Moser, K., K. Tokoyoda, A. Radbruch, I. MacLennan, and R. A. Manz.** 2006. Stromal niches, plasma cell differentiation and survival. Curr. Opin. Immunol. **18:**265–270.
45. **Mueller, S. N., et al.** 2007. Regulation of homeostatic chemokine expression and cell trafficking during immune responses. Science **317:**670–674.
46. **Muller, M., S. Carter, M. J. Hofer, and I. L. Campbell.** 2010. The chemokine receptor CXCR3 and its ligands CXCL9, CXCL10 and CXCL11 in neuroimmunity–a tale of conflict and conundrum. Neuropathol. Appl. Neurobiol. **36:**368–387.
47. **O'Connor, B. P., et al.** 2004. BCMA is essential for the survival of long-lived bone marrow plasma cells. J. Exp. Med. **199:**91–98.
48. **Owens, G. P., et al.** 2007. Measles virus-specific plasma cells are prominent in subacute sclerosing panencephalitis CSF. Neurology **68:**1815–1819.
49. **Ozaki, K., et al.** 2002. A critical role for IL-21 in regulating immunoglobulin production. Science **298:**1630–1634.
50. **Pachner, A. R., J. Brady, and K. Narayan.** 2007. Antibody-secreting cells in the central nervous system in an animal model of MS: phenotype, association with disability, and in vitro production of antibody. J. Neuroimmunol. **190:** 112–120.
51. **Pachner, A. R., L. Li, and K. Narayan.** 2007. Intrathecal antibody production in an animal model of multiple sclerosis. J. Neuroimmunol. **185:**57–63.
52. **Parra, B., et al.** 1999. IFN-gamma is required for viral clearance from central nervous system oligodendroglia. J. Immunol. **162:**1641–1647.
53. **Parsons, L. M., and H. E. Webb.** 1982. Blood brain barrier disturbance and immunoglobulin G levels in the cerebrospinal fluid of the mouse following peripheral infection with the demyelinating strain of Semliki Forest virus. J. Neurol. Sci. **57:**307–318.
54. **Parsons, L. M., and H. E. Webb.** 1992. IgG subclass responses in brain and serum in Semliki Forest virus demyelinating encephalitis. Neuropathol. Appl. Neurobiol **18:**351–359.
55. **Parsons, L. M., and H. E. Webb.** 1982. Virus titres and persistently raised white cell counts in cerebrospinal fluid in mice after peripheral infection with demyelinating Semliki Forest virus. Neuropathol. Appl. Neurobiol **8:**395–401.
56. **Phares, T. W., R. B. Kean, T. Mikheeva, and D. C. Hooper.** 2006. Regional differences in blood-brain barrier permeability changes and inflammation in the apathogenic clearance of virus from the central nervous system. J. Immunol. **176:**7666–7675.
57. **Phares, T. W., et al.** 2009. Target-dependent B7-H1 regulation contributes to clearance of central nervous system infection and dampens morbidity. J. Immunol. **182:**5430–5438.
58. **Ramakrishna, C., C. C. Bergmann, R. Atkinson, and S. A. Stohlman.** 2003. Control of central nervous system viral persistence by neutralizing antibody. J. Virol. **77:**4670–4678.
59. **Rauch, M., R. Tussiwand, N. Bosco, and A. G. Rolink.** 2009. Crucial role for BAFF-BAFF-R signaling in the survival and maintenance of mature B cells. PLoS One **4:**e5456.
60. **Rolink, A. G., and F. Melchers.** 2002. BAFFled B cells survive and thrive: roles of BAFF in B-cell development. Curr. Opin. Immunol. **14:**266–275.
61. **Rolink, A. G., J. Tschopp, P. Schneider, and F. Melchers.** 2002. BAFF is a survival and maturation factor for mouse B cells. Eur. J. Immunol. **32:**2004–2010.
62. **Savarin, C., S. A. Stohlman, R. Atkinson, R. M. Ransohoff, and C. C. Bergmann.** 2010. Monocytes regulate T cell migration through the glia limitans during acute viral encephalitis. J. Virol. **84:**4878–4888.
63. **Serafini, B., B. Rosicarelli, R. Magliozzi, E. Stigliano, and F. Aloisi.** 2004. Detection of ectopic B-cell follicles with germinal centers in the meninges of patients with secondary progressive multiple sclerosis. Brain Pathol. **14:**164–174.
64. **Serafini, B., et al.** 2010. Epstein-Barr virus latent infection and BAFF expression in B cells in the multiple sclerosis brain: implications for viral persistence and intrathecal B-cell activation. J. Neuropathol. Exp. Neurol. **69:**677–693.
65. **Shapiro-Shelef, M., and K. Calame.** 2005. Regulation of plasma-cell development. Nat. Rev. Immunol. **5:**230–242.
66. **Shulga-Morskaya, S., et al.** 2004. B cell-activating factor belonging to the TNF family acts through separate receptors to support B cell survival and T cell-independent antibody formation. J. Immunol. **173:**2331–2341.
67. **Spolski, R., and W. J. Leonard.** 2010. IL-21 and T follicular helper cells. Int. Immunol. **22:**7–12.
68. **Thangarajh, M., T. Masterman, J. Hillert, S. Moerk, and R. Jonsson.** 2007. A proliferation-inducing ligand (APRIL) is expressed by astrocytes and is increased in multiple sclerosis. Scand. J. Immunol. **65:**92–98.
69. **Tschen, S. I., et al.** 2002. Recruitment kinetics and composition of antibody-secreting cells within the central nervous system following viral encephalomyelitis. J. Immunol. **168:**2922–2929.
70. **Tschen, S. I., et al.** 2006. CNS viral infection diverts homing of antibody-secreting cells from lymphoid organs to the CNS. Eur. J. Immunol. **36:**603–612.
71. **Tyor, W. R., S. Wesselingh, B. Levine, and D. E. Griffin.** 1992. Long term intraparenchymal Ig secretion after acute viral encephalitis in mice. J. Immunol. **149:**4016–4020.
72. **Van Wagoner, N. J., and E. N. Benveniste.** 1999. Interleukin-6 expression and regulation in astrocytes. J. Neuroimmunol. **100:**124–139.
73. **Vogelzang, A., et al.** 2008. A fundamental role for interleukin-21 in the generation of T follicular helper cells. Immunity **29:**127–137.
74. **Wilms, H., et al.** 2010. Dimethylfumarate inhibits microglial and astrocytic inflammation by suppressing the synthesis of nitric oxide, IL-1beta, TNF-alpha and IL-6 in an in-vitro model of brain inflammation. J. Neuroinflammation **7:**30.
75. **Winter, O., et al.** 2010. Megakaryocytes constitute a functional component of a plasma cell niche in the bone marrow. Blood **116:**1867–1875.
76. **Zhou, J., S. A. Stohlman, N. W. Marten, and D. R. Hinton.** 2001. Regulation of matrix metalloproteinase (MMP) and tissue inhibitor of matrix metalloproteinase (TIMP) genes during JHMV infection of the central nervous system. Adv. Exp. Med. Biol. **494:**329–334.
77. **Zotos, D., et al.** 2010. IL-21 regulates germinal center B cell differentiation and proliferation through a B cell-intrinsic mechanism. J. Exp. Med. **207:** 365–378.
78. **Zuo, J., et al.** 2006. Mouse hepatitis virus pathogenesis in the central nervous system is independent of IL-15 and natural killer cells. Virology **350:**206–215.